PARAMETER OPTIMIZATION OF THE ADAPTIVE MVDR QR-BASED BEAMFORMER FOR JAMMING AND MULTIPATH SUPRESSION IN GPS/GLONASS RECEIVERS

V. Behar [1], Ch. Kabakchiev [2], G. Gaydadjiev[3], G.Kuzmanov[4], P. Ganchosov[5]
[1] Institute for Parallel Processing, Bulgarian Academy of Sciences
Acad. G. Bonchev St. 25-A, 1113 Sofia, Bulgaria
E-mail: behar@bas.bg
[2] Department of Software Technologies, Sofia University "St. Clement of Ohrid"
J. Boucher Blvd. 5, 1164 Sofia, Bulgaria
E-mail: ckabakchiev@fmi.uni-sofia.bg
[3, 4, 5] Department of Computer Engineering, Delft University of Technology
Mekelweg 4, 2628 CD Delft, the Netherlands
E-mail: g.n.gaydadjiev@ewi.tudelft.nl, G.Kuzmanov@ewi.tudelft.nl, P.N.Ganchosov@tudelft.nl

Abstract

Key words: Antenna array, GNSS, interference mitigation, STAP, Acquisition

This paper analyzes the influence of the space-time signal processing technique on the performance of GPS signal acquisition in conditions of strong broadband interference (jamming) and multipath. The space-time processing method used for effective mitigation of GPS interference before processing by a conventional acquisition algorithm is the Minimum Variance Distortionless Response beamforming method with QR factorization (MVDR QR). The numerical results obtained by simulations demonstrate that many factors such as array configuration, number of array elements, and sampling rate of the incoming data have a considerable effect on the effectiveness of both beamforming and acquisition algorithms.

Introduction

The Global Positioning System (GPS) and the Global Navigation Satellite System (GLONASS) have been designed to provide precision location estimates for various military and civilian applications. Each of the satellites transmits digitally coded data, and GPS/GLONASS receivers demodulate and process these signals from four or more satellites simultaneously in order to generate three time-difference-of–arrival estimates, allowing the user to measure the range to three satellites, and, as a result, to determine own position. Since a direct sequence spread spectrum (DSSS) signal is used in transmission, relatively low powers can be transmitted by the satellites and still to have adequate signal-to-noise-ratio (SNR) for accurate position estimation. In fact, these signals have the signal-to-noise ratio (SNR) of between -20 and -30 dB. Therefore, the key to achieve the precise position estimation performance is the processing of very weak DSSS signals from satellites that contain coarse acquisition (C/A) and precision (P) digitally coded data. Whatever, GPS/GLONASS signals have some degree of jamming protection built into the signal structure itself the weak signal strength of the received signal makes it easy for an intentional or unintentional radio frequency interference (RFI) to overcome jamming protection of the DSSS signal [1]. If a strong broadband jamming source is nearby, the receiver noise may rise to the level where the post correlation SNR of the satellite signals is below the threshold value required for tracking. Multipath is the other limiting factor in many GPS/GLONASS applications that affects both the pseudo range and carrier phase estimates. Signal multipath is the phenomenon where a satellite signal arrives at the receiver antenna after being reflected from different surfaces or buildings.

Various approaches can be used to mitigate GPS interference before signal processing in a GPS/GLONASS receiver [2]. One of them is to use different beamforming techniques for broadband nulling having in mind that the satellite signals and interfering signals usually originate from different spatial locations. The conventional (delay-and-sum) beamformer is the simplest, with all its weights of equal magnitudes and the phases that are selected to steer the array in particular direction [3]. This beamformer has unity response in each look direction, that is, the mean output power of the beamformer in the look direction is the same as the source power. In conditions of no directional interferences, this beamformer provides maximum SNR but it is not effective in the presence of directional jamming signals, intentional or unintentional. The others beamformers such as a Minimum Variance Distortionless Response (MVDR) beamformer can overcome this problem by suppressing interfering signals from off-axis directions [4]. To suppress jamming signals, this beamformer does not require the a priori information about them. It requires only the information for the direction-of-arrival of GPS signals.

In this paper, the capability of the two beamformers, conventional and MVDR, to mitigate GPS interference in order to improve the acquisition of GPS signals in conditions of jamming and multipath is studied and compared for different array configurations. The effectiveness of these beamformers is evaluated in terms of the following quality parameters – the improvement in signal-to-noise-plus-interference ratio (SINR) - at the

beamformer output and the probability of detection - at the output of the acquisition algorithm. The influence of different factors, namely array configuration, number of array elements and sampling rate of the incoming data, on the overall "beamforming + acquisition" algorithm is evaluated using the Monte Carlo approach.

2. Software-based GPS receiver

The structure of a software-based GPS receiver is shown in Fig.1. It processes signals received from the GPS satellites, which are in view, and then uses the information extracted to determine and display the user position, velocity, and time [1]. The GPS receiver is a multi-channel device, where one channel processes the incoming signal from one satellite. The first blocks of a receiver are an antenna and RF front-end devices, which are usually implemented in hardware.

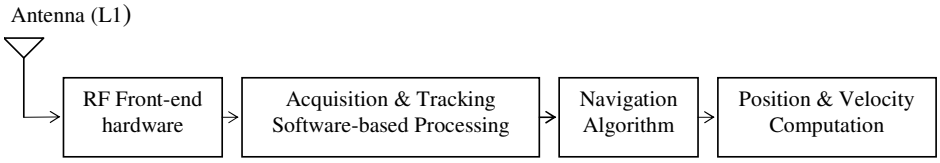

Fig.1: Architecture of a software-based GPS receiver

In the RF front-end section, the GPS signal is down converted from the RF frequency to an intermediate frequency (IF) by one of multiple stages. The down converters reduce the GPS carrier frequency from GHz to a couple MHz. The last stage of the RF front-end section is an Analog-to Digital Converter, where the IF signals are sampled at a suitable sampling frequency and digitized. In the next blocks of a GPS receiver, the satellite signal is processed in multiple (until 8 to 12) parallel channels, where each channel acquires and dynamically tracks one visible satellite. A minimum four channels tracking the signals of four satellites would be required to determine three position coordinates and the receiver clock offset. In a conventional hardware-based receiver, the last three blocks in Fig.1 are implemented in an IC chip, and the algorithms built inside the chip are not available for the user. In a software-based GPS receiver, however, these blocks are implemented in software and hence the user has a free access to the algorithms and can exercise control over them. This is the difference between the software-based GPS receiver and a conventional hardware-based GPS receiver.

3. Signal model

The GPS employs spread-spectrum (SS) techniques for transmission at two frequency bands L1 (1572.42 MHz) and L2 (1227.6 MHz). The signal transmitted at L1 contains coarse acquisition (C/A) code, precision (P) code and navigation data while the signal transmitted at L2 has P-code only. In this paper we limit discussion within the L1 band and C/A code only because the frequency band L2 and P-code serves the military purposes only and the civilian community does not have a free access to the encryption codes of P-code. The C/A code has a rate of 1.023 Mchips/s with a period of 1023 chips (1ms). The C/A code based on Gold codes is a sequence of zeros and ones, and it is unique for every satellite. The main property of the C/A code is that it has the best cross-correlation characteristic. The cross-correlation between two codes is very much lower than the auto-correlation of each of the codes. In GPS applications, when the receiver is on the ground, the input SNR value depends on the RF-bandwidth of the receiver front-end and is typically around -20dB (2.046 MHz C/A code bandwidth). The ideal received signal is composed of the GPS signal, thermal noise and a variety of interference. The complex samples of the received signal at time instant k can be mathematically described as:

$$x(k) = a_c s(k) + \sum_{l=1}^{L} b_l j_l(k) + \sum_{p=1}^{P} q_p m_p(k) + n(k) \tag{1}$$

where $x(k)$ is the M x 1 data vector, $s(k)$ is the desired GPS signal, $j_l(k)$ is the lth broadband interference, $m_p(k)$ is the pth multipath, a_c , b_l and q_p are M x 1 antenna array response vectors of the GPS signal, the lth broadband interference and the pth multipath, respectively, $n(k)$ is the noise vector and L and P is the number of broadband interference sources and multipath signals, respectively. The GPS signal is given by:

$$s(k) = \sqrt{P_s}\, c(k) d(k) \tag{2}$$

where P_s is the signal power, $c(k)$ is the C/A coded signal of length (20 x 1023), separate for each satellite, $d(k)$ is the GPS data bit which remains constant over the length of one cycle of the C/A code. The jamming signal $j(k)$ occupies the entire RF bandwidth of the GPS receiver and usually has a flat power spectrum over the passband of the GPS receiver and thus it can be represented mathematically as bandlimited white additive Gaussian noise (AWGN). The ability of the GPS receiver to perform critical functions is called as its *anti-jamming capability*, which is defined as the ratio of interference power to GPS signal power, above which the receiver function

cannot be performed. Multipath is another significant source of errors for high accuracy positioning in GPS applications. Multipath is the phenomenon whereby a signal is reflected from multiple objects in the environment and arrives at the receiver via multiple paths. According to [5], the multipath signal $m_p(k)$ in (2) can be modeled as:

$$m_p(k) = \alpha_p s(k - \delta_p) \exp(-2\pi i \Delta f_p k + i\phi_p) \tag{3}$$

where α_p is the multipath amplitude, δ_p is the delay, Δf_p is the difference between Doppler frequencies of the GPS signal and multipath. This frequency is very small since the distance and the relative speed between the mobile and reflecting surface are very small with respect to the satellite-mobile ones. According to [5], the worst situation for position estimation is when the phase Φ_p is 0° or 180°. In that case the GPS receiver can not distinguish between a direct and reflected signal, and as a result, the receiver tracking loops align the locally generated code and carrier to the composite signal instead of the direct signal causing the multipath error.

4. Antenna array geometry

Antenna arrays are composed of many antenna elements working jointly to establish a unique radiation pattern in the desire direction. The antenna elements are put together in a known geometry, which is usually uniform - Uniform Linear Arrays (ULA), Uniform Rectangular Arrays (URA) or Uniform Circular Arrays (UCA) [6, 7]. Since the ULA beam pattern can be controlled only in one dimension (azimuth), so in GPS applications, a URA configuration or a UCA configuration with the elements extended in two dimensions must be used in order to control the beam pattern in two dimensions (azimuth and elevation).

URA configuration

In a URA, all elements are extended in the *x*-*y* plane. There are M_X elements in the *x*-direction and M_Y elements in the *y*-direction creating an array of (M_X x M_Y) elements. All elements are uniformly spaced *d* apart in both directions. Such a rectangular array can be viewed as M_Y uniform linear arrays of M_X elements or M_X uniform linear arrays of M_Y elements. Usually, the first antenna element is considered as the origin of Cartesian coordinates as shown in Fig.2. The direction of a signal arriving from azimuth φ and elevation θ can be described with a unit vector *e* in Cartesian coordinates as:

$$e(\varphi,\theta) = (e_x, e_y, e_z) = (\cos\theta\sin\varphi, \cos\theta\cos\varphi, \sin\theta) \tag{4}$$

The vector in the direction of the *m(i,k)* element can be described in Cartesian coordinates as:

$$r_{m(i,k)} = (d(i-1), d(k-1), 0) \tag{5}$$

In (5), *i* and *k* denote the element position along the *y*- and the *x*-axis, respectively. The sequential element number *m(i,k)* is defined as:

$$m(i,k) = (i-1)M_X + k, \quad i = 1 \div M_Y,\ k = 1 \div M_X \tag{6}$$

If the first element in the rectangular array is a reference element, the path-length difference $d_{m(i,k)}$ for a signal incident at element *m(i,k)* can be defined as the projection of the vector $r_{m(i,k)}$ on the signal direction vector *e*:

$$d_{m(i,k)} = e^T \cdot r_{m(i,k)} = \cos\theta \cdot d \cdot [\sin\varphi(i-1) + \cos\varphi(k-1)] \tag{7}$$

Therefore, the URA response vector a_c in (1) takes the form:

$$a_c(\varphi,\theta) = [1, \exp(j\frac{2\pi}{\lambda}d_2), \ldots, \exp(j\frac{2\pi}{\lambda}d_{m(i,k)}), \ldots, \exp(j\frac{2\pi}{\lambda}d_M)], \text{ where } M=M_X \text{ x } M_Y \tag{8}$$

UCA configuration

In a UCA, all elements are arranged along the ring of radius *r* (Fig.3). The ring contains *M* array elements. Since these elements are uniformly spaced within the ring, so they have an interelement angular spacing $\Delta\varphi = 2\pi/M$ and a linear interelement spacing $d = 2r\pi/M$. It is usually assumed that the first antenna element is located at the *y*-axis, and the ring center is the origin of Cartesian coordinates. The vector in the direction of the *m*th array element can be written in Cartesian coordinates as:

$$r_m = (r\sin\varphi_m, r\cos\varphi_m, 0), \text{ where } \varphi_m = 2\pi(m-1)/M \tag{9}$$

The unit vector $e(\varphi,\theta)$ in the direction of a signal source is given by (4). If the ring center serves as a reference point, the propagation path-length difference d_m for a signal incident at element *m* can be defined as the projection of the vector r_m on the direction vector *e*:

$$d_m = e^T \cdot r_m = d \cdot \cos\theta(\sin\varphi\sin\varphi_m + \cos\varphi\cos\varphi_m) = d\cos\theta\cos(\varphi - \varphi_m) \tag{10}$$

Therefore, the UCA response vector a_c in (1) takes the form:

$$a_c(\varphi,\theta) = [\exp(j\frac{2\pi}{\lambda}d_1), \exp(j\frac{2\pi}{\lambda}d_2), \ldots, \exp(j\frac{2\pi}{\lambda}d_m), \ldots, \exp(j\frac{2\pi}{\lambda}d_M)] \tag{11}$$

where d_m is calculated by (10) for *m=1,2,...M*.

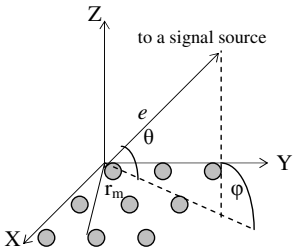

Fig.2: URA configuration

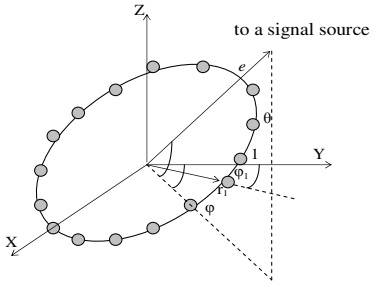

Fig.3 UCA configuration

5. GPS signal processing

The signal processing in a conventional GPS receiver includes acquisition and tracking of the GPS signal. In this paper we limit our discussion with the acquisition stage only. In our case, the GPS signal processing includes two stages (Fig.4). At the first stage the digital beamforming is performed in order to mitigate broadband interference and multipath. At the second stage the standard acquisition algorithm is performed.

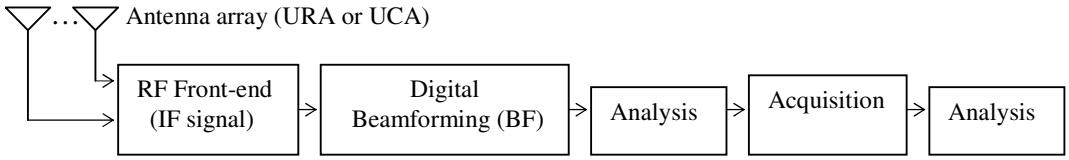

Fig.4: The flow-chart of the evaluation process

Beamforming stage

The digital beamformer increases the gain in the direction of arrival of the desired signal, and decreases the gain in all other directions (interference). The output of an antenna array of *M* elements is formed as:

$$y(k) = W^H x(k), \text{ where } k=1\ldots N \tag{12}$$

where $(.)^H$ denotes conjugate transpose.

***Conventional Beamformer*:** In a conventional beamformer, the complex vector of weights *W* is equal to the array response vector a_c, which is defined by array configuration [8]:

$$W_{conv} = a_c \tag{13}$$

***MVDR Beamformer*:** The objective of the adaptive beamforming is to preserve the gain in the direction of arrival of the desired signal and mitigate broadband interference incoming from the other directions. The weight vector W is chosen to maximize the signal-to-interference-plus-noise ratio at the antenna output [9, 10]:

$$SINR = \frac{\sigma_S^2 \left| W^H a_c \right|^2}{W^H K_{j+n} W} \tag{14}$$

where K_{j+n} is the "interference + noise" covariance matrix of size (*M x M*), and σ_S^2 is the signal power. The easy solution can be found by maintaining the distortionless response toward signal and minimizing the power at the filter output. This criterion of optimization is formulated as:

$$\min_W W^H K_{j+m+n} W \quad \text{to subject } W^H a_c = 1 \tag{15}$$

The solution of (15) is known as the minimum variance distortionless response beamformer (MVDR):

$$W_{MVDR} = \frac{K_{j+n}^{-1} a_c}{a_c^H K_{j+n}^{-1} a_c} \tag{16}$$

In practical applications, K_{j+n}, is unavailable. For that reason the sample covariance matrix $\widehat{K}$ is used instead of it. The sample covariance matrix is estimated as:

$$\widehat{K} = \frac{1}{N} \sum_{n=1}^{N} x(n) x^H(n) \tag{17}$$

Many practical applications of MVDR-beamformers require online calculation of the weights according to (16), and it means that the covariance matrix (17) should be estimated and inverted online. However, this operation is

very computationally expensive and it may be difficult to estimate the sample covariance matrix in real time if the number of samples MN is large. Furthermore, the numerical calculation of the weights W_{MVDR} using the expression (16) may be very unstable if the sample covariance matrix is ill-conditioned. A numerical stable and computationally efficient algorithm can be obtained by using QR decomposition of the incoming signal matrix. This matrix is decomposed as $X=QR$, where Q is the unitary matrix and R is the upper triangular matrix. Hence the QR-based algorithm for calculation of beamformer weights includes the following three stages:

- The linear equation system $R^H z_1 = a_c$ is solved for z_1, and the solution is $z_1^* = (R^H)^{-1} a_c$
- The linear equation system $Rz_2 = z_1^*$ is solved for z_2, and the solution is $z_2^* = R^{-1} z_1^*$
- The weight vector $\widehat{W}$ is obtained as $\widehat{W} = z_2^* / (a_c^H z_2^*)$

Acquisition stage

The main purpose of the acquisition stage is to identify the visible satellites in the incoming data and then find the beginning point of the C/A code and estimate the rough Doppler shift by correlating the incoming signal with the local signal replica. Since the C/A code is 1ms long, the acquisition must be performed on at least 1ms of the incoming data. According to [1] the acquisition algorithm consists of the following steps:

- Perform the FFT of the input data $x(k)$ converting them into frequency domain as $X(k)$.
- Take the complex conjugate $X(k)$ obtaining the outputs $X^*(k)$.
- Generate 21 local codes $l_{si}(k)$ as $l_i(k)=c(k)exp(2\pi j f_i)$, , where $f_i=f_c+i\cdot$kHz, f_c- is the intermediate frequency and i=-10,-9,….9, 10. The local code is the product of the C/A code satellite and a complex IF signal. The frequencies f_i of the local codes are separated by 1 kHz.
- Perform the FFT on $l_{si}(k)$ to transform them to the frequency domain as $L_i(k)$.
- Multiply $X^*(k)$ and $L_i(k)$ point by point obtaining the result $R_i(k)$.
- Take the IFFT of $R_i(k)$ to transform the result into time domain as $r_i(k)$ and find its absolute value $| r_i(k)|$.
- The maximum of $| r_i(k)|$ in the kth location and ith frequency bin gives the beginning point of the C/A code in $(1/f_s)$ resolution in the input data and the carrier frequency in 1kHz resolution (f_s–is the sampling frequency).

When both parameters, the beginning point of the C/A code and the carrier frequency, are found, this information is passed on to the tracking algorithm.

6. Performance measures

The performance measures presented here serve to evaluate the performance of the two beamforming techniques and select the best parameters of the space-time processing in order to provide a high degree of the acquisition efficiency. These quality measures are defined as follows:

- *SINR improvement factor* – For a single element array the input SINR is defined as:

$$SINR_{INPUT} = \frac{P_S}{P_N + P_i + P_m} \tag{18}$$

where P_S is the average power of the desired GPS signal, P_N is the receiver noise power, P_i is the total broadband jamming power, and P_m is the total multipath power. Using the superposition principle, the SINR at the beamformer output can be evaluated as

$$SINR_{OUT} = \frac{(W^H s)(W^H s)^H}{(W^H x_0)(W^H x_0)^H} \tag{19}$$

where x_0 is the total "noise + interference + multipath" signal that arrives at an antenna array element. Therefore the improvement in SINR provided by the beamformer can be found as:

$$K_{SINR} = SINR_{OUT} / SINR_{INPUT} \tag{20}$$

This quality measure evaluates the capability of the beamformer (conventional or MVDR) to cancel the interference power in the incoming signal and at the same time to preserve the desired signal power.

- *Probability of detection* (P_D) – This quality measure evaluates the capability of the overall "beamforming + acquisition" algorithm to detect the beginning point of the C/A code and find correctly the carrier frequency of the incoming IF signal. This performance measure can be evaluated using the Monte Carlo approach:

$$P_D = K_{success} / N_{total} \tag{21}$$

where

$K_{success}$ is the number of events, in which both parameters being estimated, the beginning point and the carrier frequency, are found correctly;

N_{total} is the total number of Monte Carlo runs.

7. Simulation results

In this section, 500 computer simulations of the overall "beamforming + acquisition" algorithm are performed in order to evaluate the influence of such factors as array configuration, number of array elements and sampling rate on the capability of the algorithm to operate effectively in conditions of strong broadband interference and multipath. The smallest interelement spacing in antenna arrays is usually equal to or slightly less than half a wavelength of the satellite carrier frequency ($\lambda/2$) in order to avoid the problem of "spatial under-sampling". However, a smaller interelement spacing than $\lambda/2$ increases the risk of mutual coupling between antenna elements. In GPS/GLONASS applications, the interelement spacing is approximately 0.09m for the L1-band, and this technical demand puts a physical limitation on how small the array can be used in a GPS/GLONASS receiver and how many elements is appropriate to be used in such an antenna array. For that reason we consider a limited number of array configurations, which have a small number of elements. Four examples of such arrays are presented in Table 1.

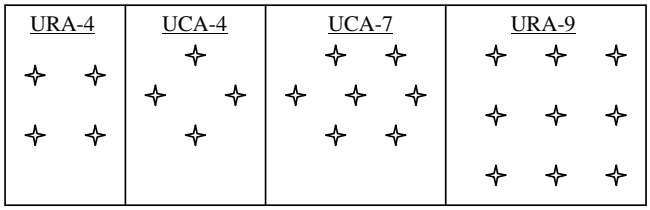

Table 1: Array configurations

The first two arrays, rectangular (URA-4) and circular (UCA-4), contain four elements with half-wavelength interelement spacing. The third of arrays is a uniform circular array with seven elements (UCA-7) where the first element is located at the array center. The radius of this array is equal to one half-wavelength. The last of arrays is a rectangular array with 9 elements. It is well known that the number of antenna elements M is related to the number of broadband jammers that can be nulled by the space-time beamforming algorithm. Typically, the number of broadband jammers that can be nulled by the space-time filtering corresponds to (M-1). With this in mind five scenarios with the main parameters described in Table 2 are simulated.

Scenario	**Jamming**	**Multipath**	**GPS signal**
Scenario 1	Receiver noise only		Elevation: θ=40° Azimuth: φ=0° Doppler shift:5 kHz SNR: -20dB Variant 1 Carrier: 1.2513 MHz Sampling:5.0053 MHz Variant 2 Carrier: 2.4967 MHz Sampling: 9.9868 MHz Duration: 1ms C/A code: satellite 19
Scenario 2	URA-4 and UCA-4 Three jamming sources: Elevation: θ=40° Azimuth: φ_1=-70°;φ_2=-60°;φ_3=60° ISR: 10dB …. 100dB	-	
Scenario 3	URA-9 and UCA-7 Four jamming sources: Azimuth: φ_4=70° ISR: 10dB … 100dB	-	
Scenario 4	-	URA-4 and UCA-4 One or three echoes: Elevation: θ=10° Azimuth: φ=Rav[-90°,-40°]& Rav[90°,40°] Attenuation: 2dB Doppler shift: 0; Phase: 0 Excess delay: 0.5 PRN chip	
Scenario 5	-	URA-4 and UCA-4 One, three or five echoes: Elevation: θ=10° Azimuth: φ=Rav[-90°,-40°]& Rav[90°,40°] Attenuation: 2dB Doppler shift: 0; Phase: 0 Excess delay: 0.5 PRN chip	

Table 2: Jamming and multipath scenarios

In the first scenario, the received signal consists of a single GPS signal and additive white Gaussian noise with unity variance. For this scenario, the estimates of the improvement in SNR evaluated by 500 simulation runs are tabulated in the first row of Table3. It can be seen that in the interference-free environment both beamformers have the same improvement in SNR. The second scenario, in which where three broadband jamming signals are added to the GPS signal and noise, is simulated with four-element arrays: URA-4 and UCA-4. Analogically, the third scenario, in which four jamming signals are combined with the GPS signal and noise, is simulated with arrays URA-9 and UCA-7. For all these arrays, the estimates of the improvement in SINR are evaluated as a function of the interference-to-signal ratio (ISR) (Table 3). Numerical results given in Table 3 are plotted in Fig. 5 – for URA-4 and UCA-4 and in Fig.6 – for URA-9 and UCA-7.

ISR (dB)	SINR Improvement (dB)							
	Conventional Beamformer				MVDR Beamformer			
	URA-4	UCA-4	URA-9	UCA-7	URA-4	UCA-4	URA-9	UCA-7
-	3.01	3.01	6.54	5.44	3.01	3.01	6.54	5.44
10	3.45	3.95	7.99	6.79	3.53	4.01	7.99	6.82
20	4.65	7.4	13.45	11.42	6.31	8.33	13.49	11.85
30	5.27	10.46	22.00	15.98	13.26	14.62	22.60	19.7
40	5.36	11.10	28.40	17.13	22.21	21.21	32.50	29.04
50	5.37	11.17	30.23	17.26	31.99	30.35	42.48	38.95
60	5.37	11.17	30.46	17.28	41.97	40.24	52.48	48.94
100	5.37	11.17	30.49	17.28	81.97	80.23	92.48	88.94

Table 3: SINR Improvement evaluated for the two beamformers

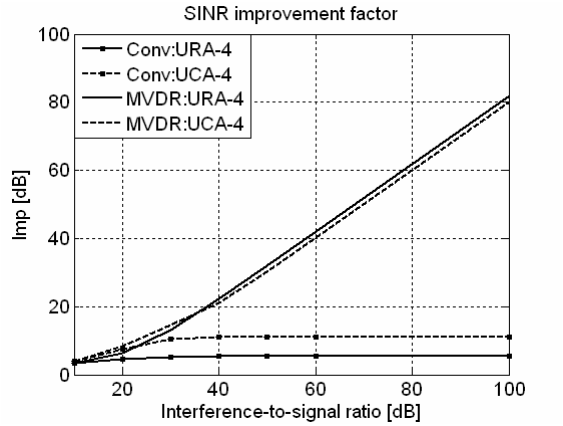

Fig. 5: SINR improvement for URA-4 and UCA-4

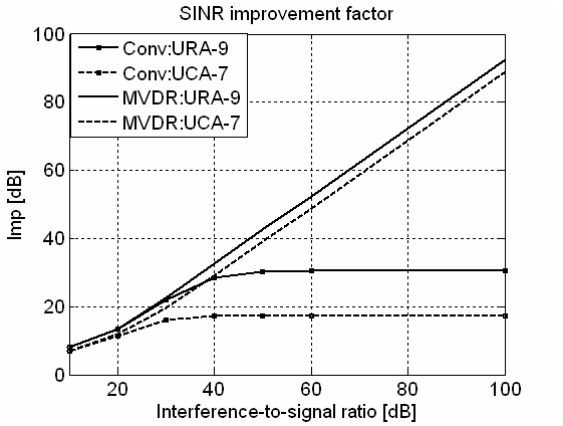

Fig. 6: SNR improvement for URA-9 and UCA-7

The antenna pattern of the UCA-7 calculated for the case of four strong jamming signals (ISR =60 dB) is shown in Fig.7. The minimal gain is created in the direction of arrival of jamming signals (-70°,-60°, 60°, 70°) while the maximal gain is created in the direction of the GPS signal (0°). The correlator outputs are plotted in Fig. 8.

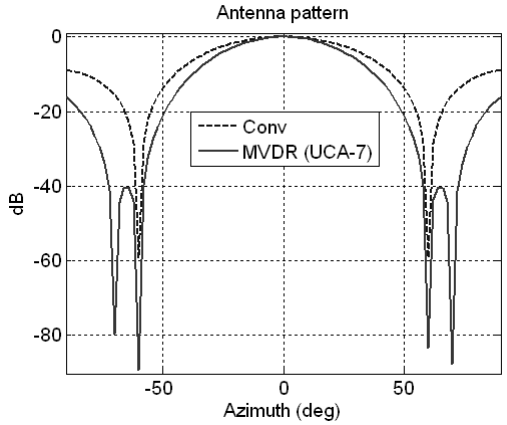

Fig. 7: Antenna pattern (4 jammers, ISR =60 dB)

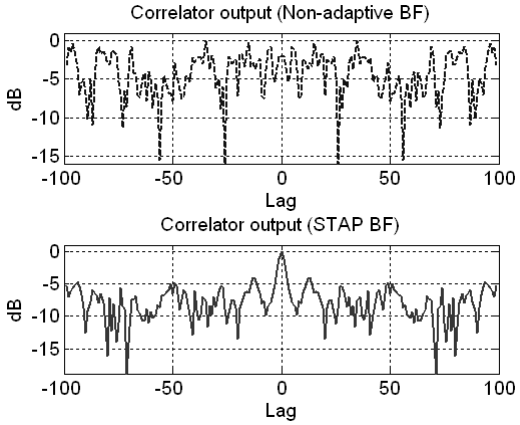

Fig. 8 Correlator output (UCA-7, 4 jammers, ISR =60dB)

As is shown above, the capability of each of the two beamformers to suppress broadband interference depends not only on the array geometry - URA and UCA but the number of array elements as well - 4, 7, 9. However, unlike the conventional beamformer the MVDR-beamformer very successfully mitigates broadband interference even if the interference intensity becomes 100 dB over the desired GPS signal. The MVDR-beamformer achieves the most effect for URA-9. As whole, the rectangular array configuration is more effective for broadband interference suppression than circular one. The effectiveness of the overall "beamforming + acquisition" algorithm can be estimated in terms of the detection probability, which is defined as the probability of an event in which both parameters of the incoming GPS signal, the beginning point and the carrier frequency, are correctly estimated. The detection probability is calculated using 500 simulation runs. The probability of detection is estimated for two values of the sampling frequency of the incoming data. The estimates obtained are presented in Table 4 – for URA-4 and UCA-4 and in Table 5 – for URA-9 and UCA-7. The analogical graphical results are plotted in Fig. 9, 10, 11 and 12.

ISR (dB)	**Probability of detection (P_D)**							
	Sampling frequency (5.0053 MHz)				**Sampling frequency (9.9868 MHz)**			
	Conventional Beamformer		**MVDR QR Beamformer**		**Conventional Beamformer**		**MVDR QR Beamformer**	
	URA-4	**UCA-4**	**URA-4**	**UCA-4**	**URA-4**	**UCA-4**	**URA-4**	**UCA-4**
-	1	1	1	1	1	1	1	1
10	**0.992**	1	0.992	1	1	1	1	1
20	0.854	**0.990**	**0.974**	0.994	**0.952**	**0.996**	0.984	0.996
30	0.008	0.288	0.796	**0.954**	0.058	0.694	**0.94**	**0.976**
40	0	0	0.630	0.410	0	0.008	0.898	0.826
50	0	0	0.572	0.264	0	0	0.894	0.696
60	0	0	0.571	0.256	0	0	0.882	0.670
100	0	0	0.570	0.252	0	0	0.872	0.670

Table 4: Probability of detection evaluated for URA-4 and UCA-4

In Table 4 and Table 5, the ISR values that correspond to the probability of detection above 0.9 (noted in bold) can characterize the anti-jamming capability of the overall "beamforming + acquisition" algorithm. The estimates in Table 4 show that the MVDR-beamformer increases the antijamming capability of the acquisition algorithm by 10dB compared to the conventional beamformer.

ISR (dB)	**Probability of detection (P_D)**							
	Sampling frequency (5.0053 MHz)				**Sampling frequency (9.9868 MHz)**			
	Conventional Beamformer		**MVDR QR Beamformer**		**Conventional Beamformer**		**MVDR QR Beamformer**	
	URA-9	**UCA-7**	**URA-9**	**UCA-7**	**URA-9**	**UCA-7**	**URA-9**	**UCA-7**
-	1	1	1	1	1	1	1	1
10	1	1	1	1	1	1	1	1
20	1	1	1	1	1	1	1	1
30	1	**0.95**	1	1	1	**0.962**	1	1
40	**0.992**	0.018	1	1	**0.994**	0.094	1	1
50	0.112	0	1	0.998	0.438	0	1	1
60	0	0	1	0.998	0	0	1	1
100	0	0	**1**	**0.998**	0	0	**1**	**1**

Table 5: Probability of detection evaluated for URA-9 and UCA-7

According to the results from Table 4 and Table 5, the increase of the sampling frequency improves the anti-jamming protection of the acquisition algorithm only in case of URA-4 (Fig.9 and Fig.10) while for the other arrays (UCA-4, URA-9 and UCA-7) the effect of the sampling frequency on the anti-jamming capability of the acquisition algorithm is insignificant. Taken as a whole, the anti-jamming capability of the acquisition algorithm entirely depends on the effectiveness of the beamforming algorithm. The graphics in Fig.11 and Fig.12 clearly illustrate that the acquisition algorithm ensures save operation in conditions of very strong jamming signals if the MVDR-beamforming is a preliminary to acquisition.

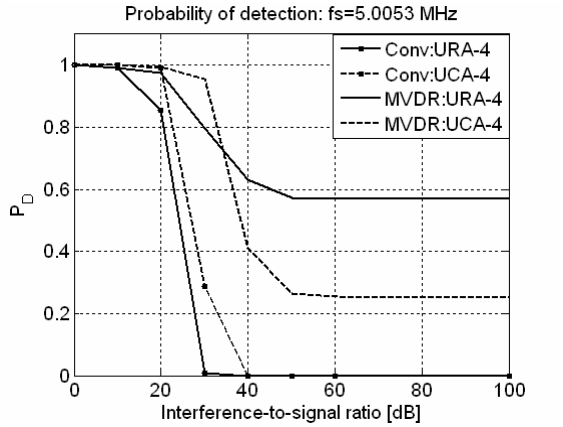

Fig. 9: Detection probability (URA-4 and UCA-4)

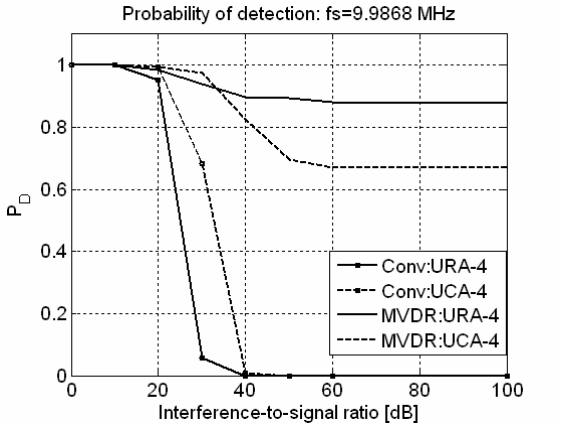

Fig. 10: Detection probability (URA-4 and UCA-4)

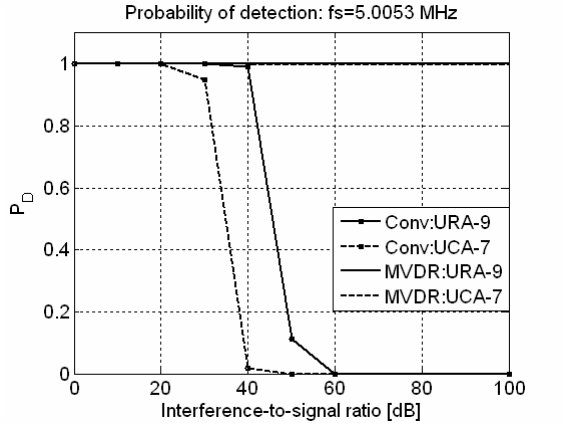

Fig. 11: Detection probability (URA-9and UCA-7)

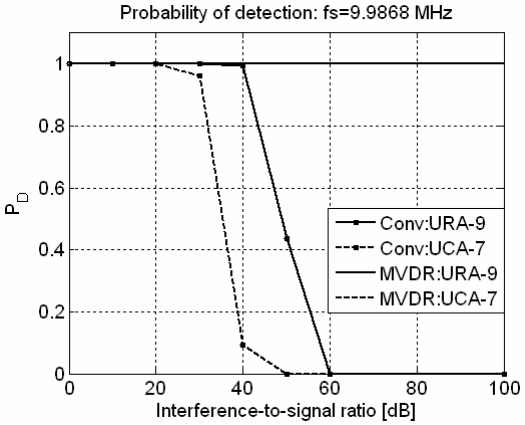

Fig. 12: Detection probability (URA-9and UCA-7)

The last two scenarios with the parameters given in Table 2 describe such an environment when multipath signals arrive at the receiver input in combination with the GPS signal. Scenario 4 is the case when one or three multipath signals are present in the received signal while scenario 5 is the case when one, three or 5 multipath signals are combined with the desired GPS signal. In simulations, it is assumed that the direction of arrival of each multipath is a random variable uniformly distributed in range [-90°,-40°] and [90°, 40°]. For these scenarios, the detection probability estimated by simulations is tabulated in Table 6. When five multipath signals are present at the receiver input, the signals at the correlator outputs are depicted in Fig. 13 and Fig. 14.

Number of echoes	**Probability of detection (P_D)**							
	Acquisition (Conventional Beamformer)				**Acquisition (MVDR QR Beamformer)**			
	URA-4	**UCA-4**	**UCA-7**	**URA-9**	**URA-4**	**UCA-4**	**UCA-7**	**URA-9**
-	1	1	1	1	1	1	1	1
1	0.999	0.962	0.998	1	0.999	0.961	0.998	1
3	0.996	0.369	0.904	1	0.998	0.401	0.964	1
5	-	-	0.450	1	-	-	0.774	1

Table 6: Probability of detection evaluated for two beamformers and two array configurations

Analysis of the results in Table 6 shows that in both cases, with the conventional beamformer and with the MVDR-beamformer, the acquisition performance degrades with increasing of the number of multipath signals. One can see that the MVDR-beamformer has no discernible advantage over the conventional one in the multipath environment. In such environment, the key advantage gives the usage of rectangular array configurations (URA-4 and URA-9) because these arrays allow maintaining a more stable operation of the acquisition algorithm in conditions of multipath. However this is not true for circular array configurations.

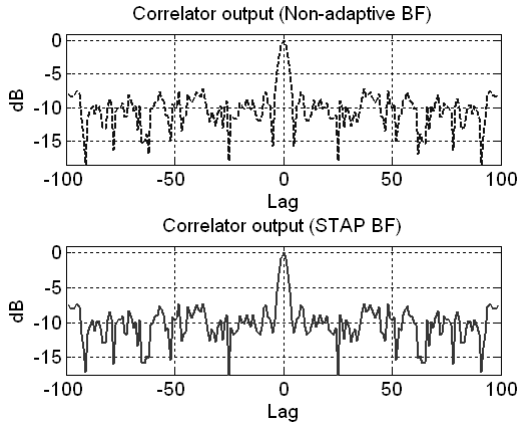

Fig. 13: Correlator output (URA-9, 5multipath)

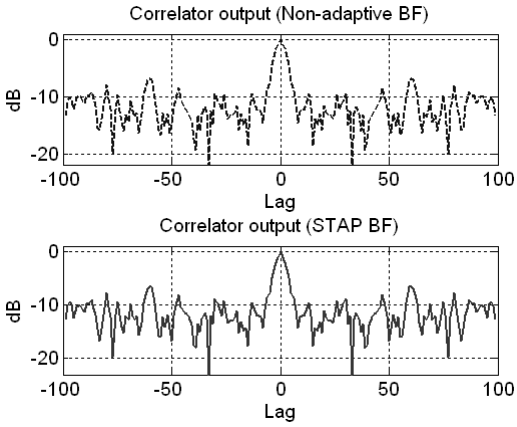

Fig. 14: Correlator output (UCA-7, 5multipath)

Conclusion

The results obtained show that the stable acquisition of GPS signals depends on several important factors when strong broadband interference and multipath signals are present at the receiver input. In the first place the effectiveness of the acquisition algorithm depends on the capability of the beamforming module to effectively suppress jamming signals and multipath before processing by the acquisition algorithm. In this context, the adaptive MVDR-algorithm is the preferable algorithm for mitigation of jamming signals. It is also shown that the physical array configuration has a very significant effect on the overall acquisition performance. In order to keep the size of arrays and beamforming complexity small, only array configurations with a small number of elements have been considered in the paper. Four different array configurations are compared in both interference-free and multi-interference environments. The results show a very good anti-jamming capability of all arrays if the MVDR-algorithm is used for beamforming. On that score the best results, however, are obtained for two rectangular arrays. As for the sampling rate of the incoming data, the influence of this factor is significant in case of arrays with a small number of elements (URA-4 and UCA-4). For arrays with a larger number of elements (URA-9 and UCA-7) this influence is insignificant.

Acknowledgment

This work is partially supported by the Bulgarian Science Fund (the project MI-1506/05 and the project MU-FS-05/2007)

Reference

1. James Bao-Yen Tsui, *Fundamentals of Global Positioning System Receivers: A Software Approach*, Wiley Interscience, John Wiley&Sons, 2005
2. J. Sklar, "Interference mitigation approaches for the Global Positioning System", *MIT Lincoln Laboratory Journal*, vol.14, No 2, 2003, 167-177
3. H. L. Van Trees, Optimum Array Processing. Part IV of Detection, Estimation, and Modulation Theory. New York, NY: JohnWiley and Sons, Inc., 2002.
4. Z.Fu, A. Hombostel, J. Hammesfahr, A. Konovaltsev, " Suppression of multipath and jamming signals by GPS/Galileo applications", GPS Solutions, No 6, 2003, 257-264
5. J. Soubielle, I. Fijalkow, P. Duvau and A. Bibaut, "GPS positioning in a multipath environment" , IEEE Trans. on Signal Processing, vol. 50, No 1, 2002, 141-150
6. D.Moelker, E. van der Pol, "Adaptive antenna arrays for interference cancellation in GPS and GLONASS receivers", *Proc. IEEE 1996 Position Location and Navigation symp*, Apr. 1996, 191-196
7. J.Lee, L.Song, J. Joung, "Uniform circular array in the parameter estimation of coherently distributed sources", *Proc. IEEE Military Communications Conf. MILCOM'2002.,*Oct.,2002,vol.2, 1258-1262
8. R. Monzingo and T. Miller, *Introduction to Adaptive Arrays*, New York: Wiley, 1980
9. L. Tummonery, I. Proudler, A. Farina, J. McWhirter, "QRD-based MVDR algorithm for adaptive multi-pulse antenna array signal processing", in *Proc. Radar, Sonar, Navigation,* vol.141, No 2, 1994, 93-102
10. P. Vouras, B. Freburger, "Application of adaptive beamforming techniques to HF radar", *in Proc. IEEE conf. RADAR'08*, May, 2008, 6.